

MULTICOMPONENT DIFFUSION IN CLAYS

CAJ Appelo¹

(1) Hydrochemical Consultant. Amsterdam

ABSTRACT

Transport processes in clays are difficult to quantify but are a key-point for deducing the properties of these materials for waste containment. To improve the situation, version 2.13 of PHREEQC was extended with multicomponent diffusion and anion exclusion in a diffuse double layer. With it, both laboratory and *in-situ* diffusion experiments can be modeled in a comprehensive manner. Application examples are discussed, and an experiment in Opalinus Clay in Mont Terri (investigated in the framework of possible storage of nuclear waste in Switzerland) is presented.

Key words: Clays, multicomponent diffusion, PHREEQC, Mont Terri experiment

1. INTRODUCTION

Clays have rather ideal properties for waste containment in the field, but the transport processes are still difficult to quantify precisely. The dominant transport mode is diffusive and different porewater diffusion coefficients have been measured for various solutes. However, almost all the models calculate transport in clays assuming that one and the same diffusion coefficient applies for all the solutes. Precipitation reactions are usually calculated assuming equilibrium, but this gives wrong results that would have been noted immediately if the model discretization had been changed. Finally, the transport properties of clays are dependent on the extent of the double layer that envelops the clay minerals, but again, this well-accepted feature is not yet accounted for in geochemical transport models.

Version 2.13 of the hydrogeochemical transport model PHREEQC (Parkhurst and Appelo, 1999) has been extended with a multicomponent diffusion module that may offer some improvement (Appelo and Wersin, 2007). The impetus was provided by detailed diffusion experiments in Opalinus Clay with various tracers (Wersin *et al.*, 2004). The basic theory for calculating multicomponent diffusion with a zero charge flux is presented, and various application examples are given.

2. MULTICOMPONENT DIFFUSION

Fick's laws calculate diffusion from concentration gradients and divergences. However, a more general equation would employ the electrochemical potential μ , rather than the concentration. The electrochemical potential is:

$$\mu = \mu^0 + RT \ln a + zF\psi \quad (1)$$

where μ^0 is the standard potential (J/mol), R is the gas constant (8.314 J/K/mol), T is the absolute temperature (K), a is the activity (-), z is the charge number (-), F is the Faraday constant (96485 J/V/eq), and ψ is the potential (V). The activity is related to concentration by $a = \gamma c/c^0$, where γ is the activity coefficient (-) and c^0 is the standard state (1 mol/kg H₂O, assumed equal to 1 mol/L in the following).

The diffusive flux of species i in solution as a result of chemical and electrical potential gradients is:

$$J_i = - \frac{u_i c_i}{|z_i| F} \frac{\partial \mu_i}{\partial x} - \frac{u_i z_i c_i}{|z_i|} \frac{\partial \psi}{\partial x} \quad (2)$$

where J_i is the flux of species i (mol/m²/s), and u_i is the mobility in water (m²/s/V). The mobility is related to the tracer diffusion coefficient $D_{w,i}$ (m²/s) by:

$$D_{w,i} = \frac{u_i RT}{|z_i| F} \quad (3)$$

The gradient of the electrical potential ($\partial\psi/\partial x$) in Equation (2) originates from different transport velocities of ions, which creates charge and an associated potential. This electrical potential may differ from the one used in Equation (1), which comes from a charged surface and is fixed, without inducing electrical current.

If there is no electrical current, $\sum z_i J_i = 0$. This zero-charge flux condition permits to express the electrical potential gradient as a function of the other terms in Equation (2) and to obtain (Vinograd and McBain, 1941; Ben-Yaakov, 1972, Cussler, 1984):

$$J_i = - D_{w,i} \left(\frac{\partial \ln(\gamma_i)}{\partial \ln(c_i)} + 1 \right) \frac{\partial c_i}{\partial x} + D_{w,i} z_i c_i \frac{\sum_{j=1}^n D_{w,j} z_j \left(\frac{\partial \ln(\gamma_j)}{\partial \ln(c_j)} + 1 \right) \frac{\partial c_j}{\partial x}}{\sum_{j=1}^n D_{w,j} z_j^2 c_j} \quad (4)$$

where subscript j is introduced to show that these species stem from the potential term.

Equation (4) looks formidable, but inspecting it piecewise will show that the terms involved are known: they consist of charge numbers and diffusion coefficients (which can be constants at a given time and place), and concentrations and activity coefficients (which are given by the space discretization of the model). Thus, the flux of any solute species can be calculated at any time, iteration (for maintaining electrical neutrality) is not necessary. The equation is valid even if the solution is not electrically neutral since any charge imbalance that may exist (notably in the diffuse double layer) is maintained by the zero-charge flux condition. The zero-charge and electroneutrality conditions have led to discussions in the geochemical literature that ended up pointless (Boudreau *et al.*, 2004).

2.1. An example: uphill diffusion (after Lichtner, 1995)

We fill a tube with 0.1 mM NaCl and 0.1 mM HNO₃ solution, the pH is 4. We make another solution with the same NaCl concentration, but with 0.001 mM HNO₃, the pH is 6. This is the boundary solution with constant concentrations over time, shown in Figure 1. The figures are copies of the charts from PHREEQC for Windows, transformed into grayscale, and clearer by coloring when run on the computer; input-files are available on request to the author, appt@xs4all.nl.

Obviously, H⁺ and NO₃⁻ are going to diffuse from the column. On the other hand, the concentration gradients of Na⁺ and Cl⁻ are zero ($dc/dx = 0$), and their concentrations remain constant according to Fick's law. The concentration pattern that results after 1 hour diffusion according to Fick is shown in Figure 2.

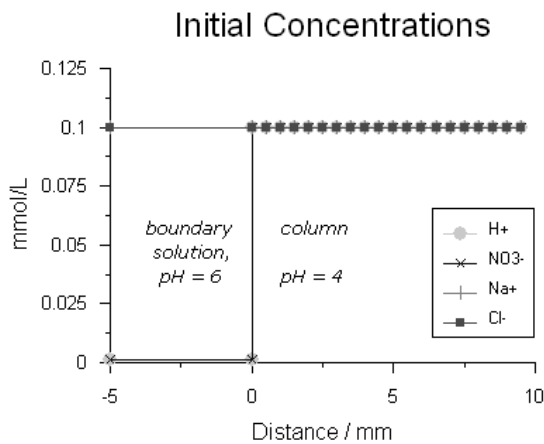


Figure 1. Initial conditions in a column example of multicomponent diffusion. The NaCl concentration is the same in the boundary solution and in the column; the concentration of HNO₃ in the column is the same as NaCl (pH = 4, symbols overlap), but 100 times lower in the boundary solution (pH = 6).

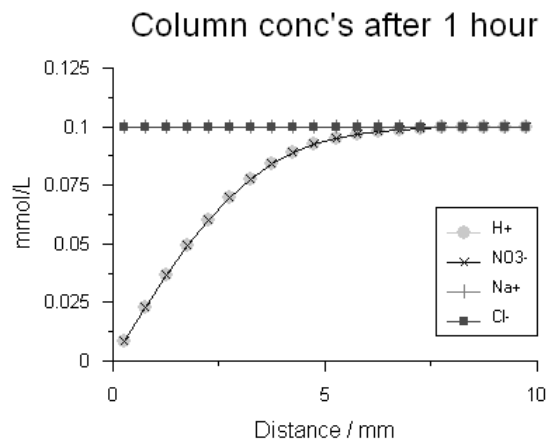


Figure 2. Concentrations in the column after 1 hour diffusion calculated according to classical diffusion (Fick) theory. Note that the concentrations of H⁺ and NO₃⁻ decrease by diffusion, while Na⁺ and Cl⁻ remain constant.

However, the diffusion coefficient of H⁺ is about 5 times higher than of NO₃⁻, and we can expect that H⁺ diffuses quicker from the column. The effect can be modeled with PHREEQC's multicomponent diffusion module, in which all the solutes diffuse according to their own diffusion coefficient. The resulting concentration pattern in Figure 3 shows indeed that more H⁺ has diffused out of the column than in the previous case. Remarkable in Figure 3 is also, that the Na⁺ concentration bulges upward, although the initial concentration gradient was zero everywhere. On the other hand, the Cl⁻ concentration has decreased, despite the initially zero concentration gradient which, according to Fick's first law, gives a zero flux.

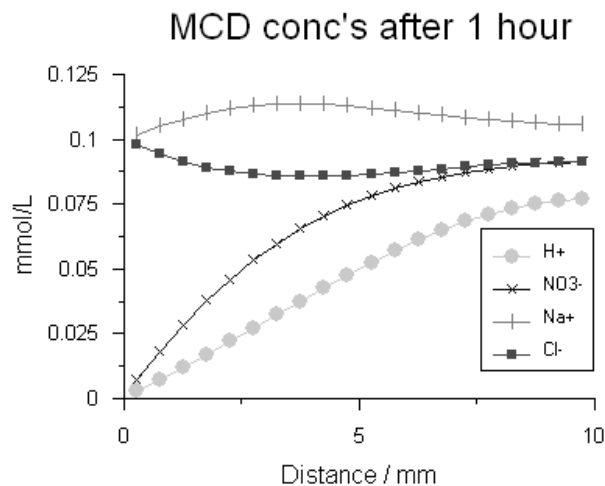


Figure 3. Concentrations in the column after 1 hour diffusion calculated with multicomponent diffusion theory.

These results can be explained as follows. After some time, the column contains more NO₃⁻ than H⁺. Na⁺ that enters the column, and Cl⁻ which leaves the column balance the resulting negative charge. The diffusion of Na⁺ and Cl⁻ starts although the initial concentration gradient is zero, and continues even against the concentration gradient that develops. This is a consequence of the zero charge flux condition that is used to calculate multicomponent diffusion. It is of interest to note that the final stage in the column, when all the concentrations are equal to the ones in the boundary solution, is reached quicker with multicomponent diffusion.

3. PRECIPITATION REACTIONS IN DIFFUSION CALCULATIONS. EFFECTS OF GRID-SIZE

Numerical models must be checked, if possible, by comparing with an analytical solution. Another, easier test is to change the gridsize and timestep. But, it has not been well appreciated that the grid size affects the results of diffusion calculations if equilibrium is assumed with solid phases. To understand what is going on, let's model an experiment of Pina *et al.* (2000), who precipitated scheelite (CaWO_4) in a column by letting CaCl_2 and Na_2WO_4 solutions diffuse from the column ends over 30 days (Figure 4).

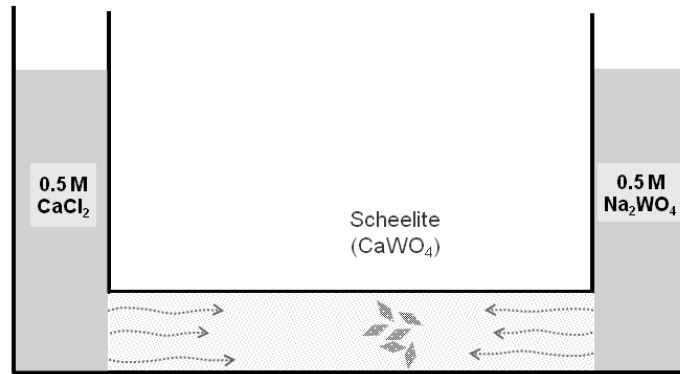


Figure 4. The setup of the diffusion experiment of Pina *et al.* (2000) in which scheelite precipitates by diffusion of Ca^{2+} and WO_4^{2-} from the two column-ends.

First, the calculation is done with classical diffusion theory, *i.e.* all the solutes diffuse at the same speed and scheelite precipitates to equilibrium where supersaturation is reached, which happens almost exclusively in the center-cell (Figure 5). With 10 mm cells, 0.09 L scheelite precipitates per L pore water; with 3.33 mm cells, the amount increases to 0.27 L, and so on. The relative amount of scheelite in the center-cell increases continuously when the grid is further refined. If the cell-size is decreased to 1 mm, the amount of scheelite will exceed the pore volume, which is of course impossible.

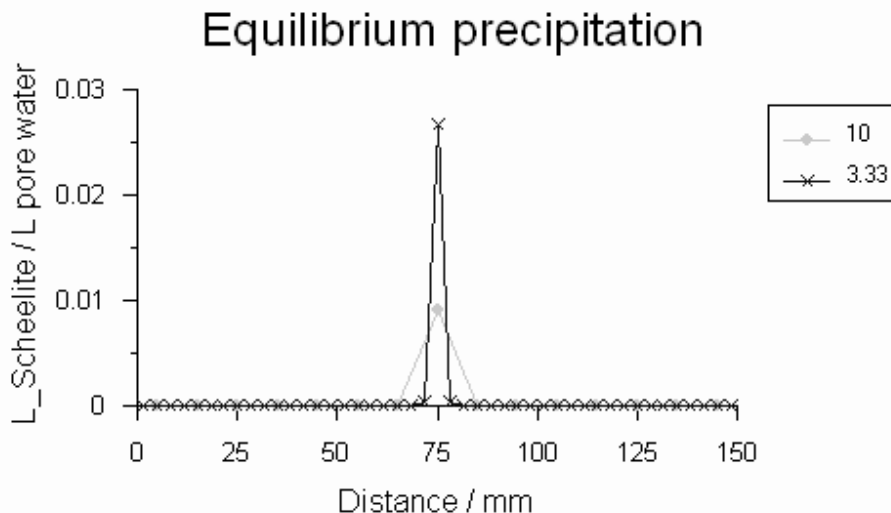


Figure 5. Precipitation of scheelite to equilibrium in a diffusion experiment calculated with 10 mm and 3.33 mm grid cells and the same diffusion coefficient for all solutes. Precipitation takes place in the center cell, irrespective of the grid size, and relative amounts increase indefinitely as the grid is refined.

The situation improves if the calculation is done with a kinetic precipitation rate that is sufficiently slow to let the solutes pass the center cell and precipitate further away. The results then become independent of grid refinement, as illustrated in Figure 6.

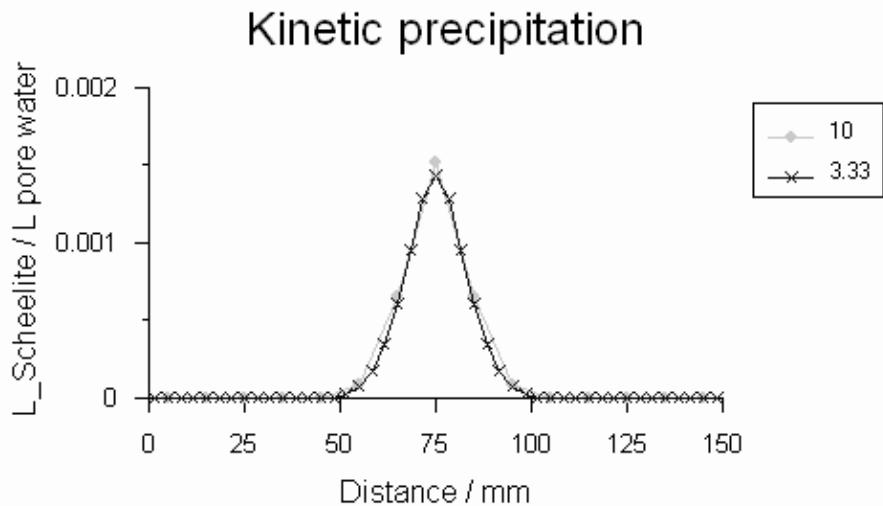


Figure 6. Precipitation of scheelite becomes independent of grid size if a kinetic rate is used that allows solutes to pass the center cell.

Kinetics is required in the model anyhow, since scheelite did not precipitate to equilibrium in the experiment. Pina *et al.* (2000) observed that precipitation occurred only when the solute ratios of Ca^{2+} and WO_4^{2-} were within certain limits. Apparently, a high supersaturation, as result of a high concentration of only one component, is insufficient to engender precipitation if the concentration of another component that is needed in the precipitate is too small. Pina *et al.* also found that the zone with scheelite was displaced away from the center towards the column end where the Na_2WO_4 solution entered. Similar features were noted already for other minerals by Prieto *et al.* (1990, 1997).

A kinetic rate was defined in the PHREEQC input file that started the homogeneous precipitation of scheelite when the saturation ratio attained 10^4 (Pina *et al.*), and when the activity ratio $[\text{Ca}^{2+}] / [\text{WO}_4^{2-}]$ ranged from 0.1 to 10. The latter requirement gives a block-like precipitation zone without the tailing that is visible in Figure 6. The off-center displacement of the precipitation zone was modeled with multicomponent diffusion, adjusting the tracer diffusion coefficient of WO_4^{2-} to $2.5 \times 10^{-10} \text{ m}^2/\text{s}$, or about 3 times smaller than of Ca^{2+} . The results in Figure 7 agree pretty well with Pina's experiment. It can be noted in passing, that the diffusion coefficients in PHREEQC are adjusted as a function of the porosity, and that the porosity is adapted according to the volume of scheelite that precipitates.

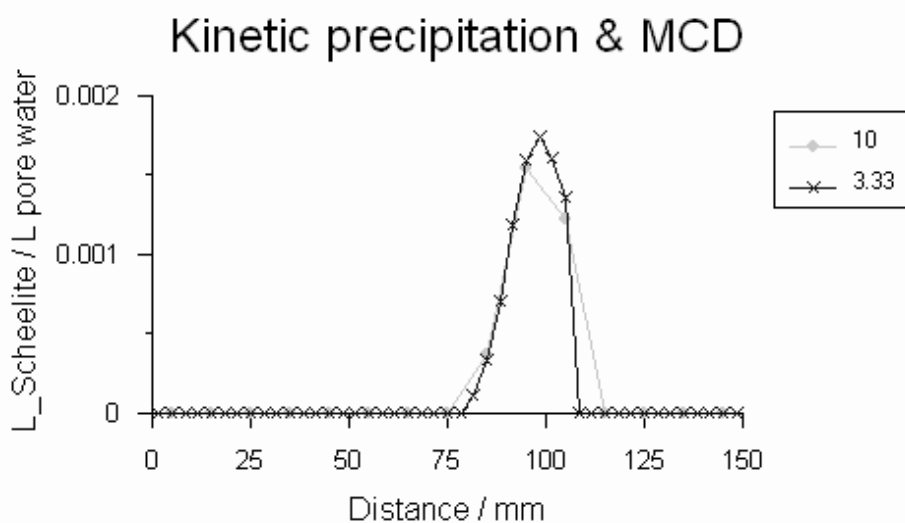


Figure 7. Modeling Pina *et al.*'s experiment with kinetic precipitation of scheelite and multicomponent diffusion. The diffusion coefficient of WO_4^{2-} is lower than of Ca^{2+} , which shifts the precipitation zone towards the column end where WO_4^{2-} enters. The curves are for 2 discretizations.

4. DIFFUSE DOUBLE LAYER EFFECTS ON DIFFUSION IN CLAYS

So far, the tracer diffusion coefficients found in plain water were used in the calculations, but abundant evidence shows that the diffusion coefficients of cations, anions and neutral species in porewater in clays have different values, and that the mutual ratios of the coefficients are dissimilar as well. Also, the accessible porosity varies and depends on the ion's charge number. It is attributed to the diffuse double layer (DDL) around the negatively charged clay, where the concentrations of anions are reduced and of cations increased. If part of the pore space is inaccessible for anions, diffusion is diminished; if the cations are at a higher concentration, their diffusion is enhanced since diffusion fluxes are coupled to concentrations as illustrated in Figure 8.

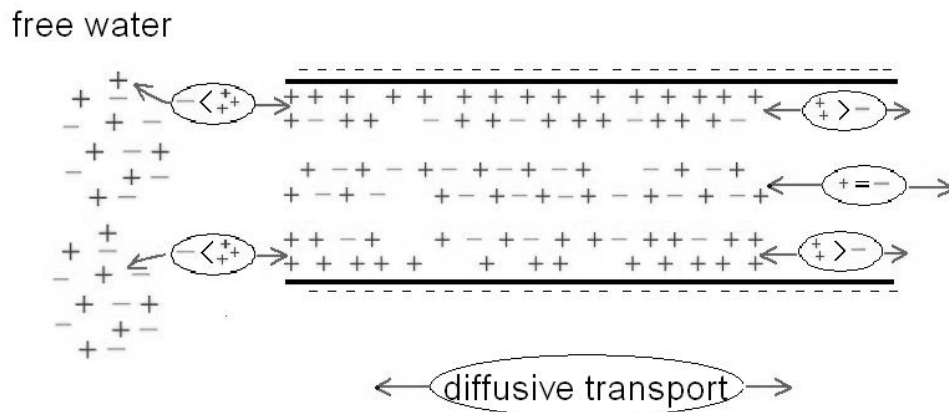


Figure 8. A pictorial simplification of solute diffusion in a (partly) charged pore connected with a free solution. Anions are excluded from the diffuse double layer at the negatively charged surface, cations are enriched there, and consequently, their diffusion is enhanced.

The DDL can be explicitly considered in PHREEQC's multicomponent diffusion calculations (Appelo and Wersin, 2007). The calculation scheme follows a discretization of Figure 8, shown in Figure 9. The pore is discretized along its length in paired cells. One cell of each pair contains a free solution that is charge-balanced; the other holds a charged surface together with the DDL. The solutes in the DDL are calculated with Boltzmann's formula, using the activities in the free porewater solution and a potential that is optimized to give zero charge of the cell (the Donnan approximation). The paired cells are aligned along the pore, and multicomponent diffusive transport is calculated by explicit finite differences for each interface among the pairs of cells.

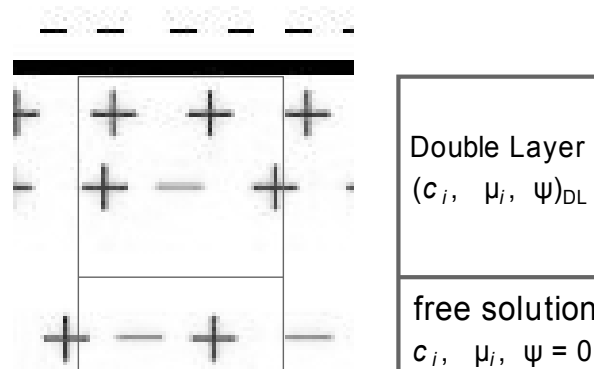


Figure 9. Discretization of a pore with a charge-free solution and a diffuse double layer that forms the basis for the multicomponent diffusion model in PHREEQC.

4.1. An example: diffusion of LiBr

An example, let's calculate the diffusion of LiBr in a diffusion cell as has been used, among others, by Sato *et al.* (1992). The two halves of the cell are filled with a porous medium, a cocktail with various tracers is distributed on the surface of one, and the two halves are clamped together. After some time, the cell is opened, sliced in parts and analyzed. Depending on the characteristics of the porous medium, and for a sample with a low cation exchange capacity (low clay content) the results may vary as illustrated in Figure 10.

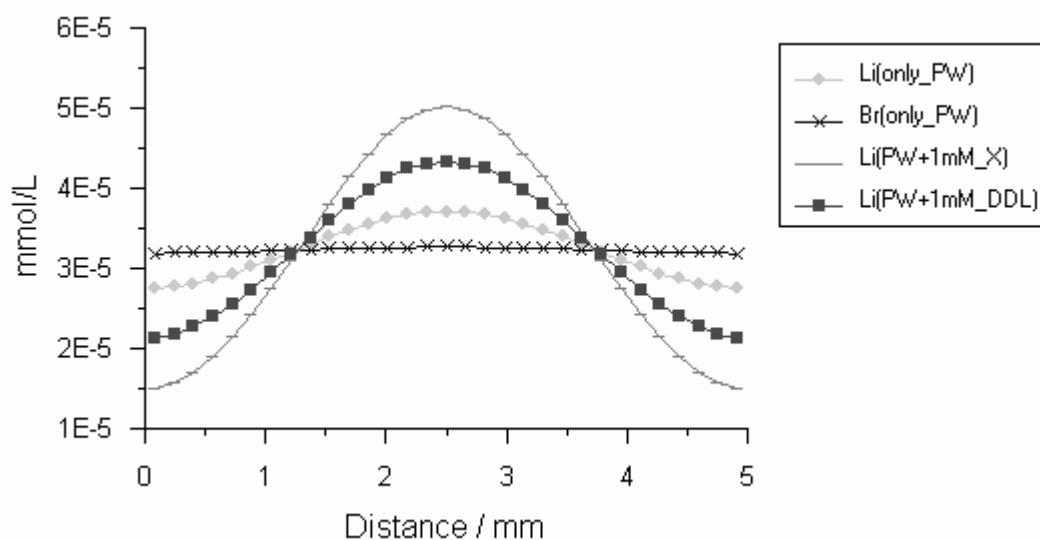


Figure 10. Diffusion of LiBr-tracer from the center of a 5 mm long diffusion cell in 30 minutes. Shown are the sum of solute and exchangeable concentrations expressed per L porewater. The calculated results are for a porous medium without cation exchange (only_PW) or with an exchange capacity of 1 mM X^- , in which the cations are either immobile on the exchanger (PW + 1 mM X) or mobile in the DDL (PW + 1 mM DDL). The porewater contains 1 mM NaCl as background electrolyte.

The diffusion coefficient of Br^- is twice higher than of Li^+ , which shows up in a larger spread of Br^- if the retardation is 1 for both ions (*i.e.* if the porous medium lacks exchange capacity, Figure 10, curves labeled as only_PW). If the medium is given an exchange capacity of 1 mM X^- , the diffusion of Li^+ is retarded by cation exchange with Na^+ , and the spread of Li^+ is further diminished (curve labeled as PW + 1 mM X). If the exchangeable cations reside in a DDL that occupies half of the pore space and can diffuse there, the spread is increased again (curve labeled as PW + 1 mM DDL). Diffusion is enhanced still further when the option is invoked that the DDL is filled with counter ions only.

The Br^- concentration pattern is hardly affected by introducing cation exchange, because in this example it concerns a given amount of chemical that has been introduced in the clay. However, diffusion of anions is notably diminished if they are coming from an outer, boundary solution and a significant part of the pore space is occupied by the DDL and thus inaccessible for anions.

5. DIFFUSION EXPERIMENTS IN OPALINUS CLAY

The Opalinus Clay, a clay-rock formation in Switzerland, is investigated for possible storage of nuclear waste, and its diffusion characteristics are probed in detailed experiments. In the *in-situ* experiments, a solution with the general composition of the formation's porewater, supplemented with various tracers, is recirculated in a borehole (Wersin *et al.*, 2004). The tracers diffuse radially outward into the formation, and the concentration changes in the borehole fluid are followed in time.

The borehole of the experiment to be discussed is inclined with respect to the bedding planes, which causes the spreading pattern to become elliptical. Accordingly, an elliptical grid is to be constructed for modeling the concentration changes with finite differences. In the following, the formulas to be used will be explained for a cylindrical grid since analytical solutions can be derived for that case. Next, the experimental concentrations are compared with the results of computations with the elliptical grid.

5.1. Finite differences for diffusion in polar coordinates

We want to solve Fick's equation in polar coordinates (r, θ):

$$\frac{\partial c}{\partial t} = D_e \left(\frac{\partial^2 c}{\partial r^2} + \frac{1}{r} \frac{\partial c}{\partial r} + \frac{1}{r^2} \frac{\partial^2 c}{\partial \theta^2} \right) \quad (5)$$

where c is concentration (mol/L), t is time (s), D_e is effective diffusion coefficient (m²/s), r is radial distance (m), θ is the angle (degrees). For the radially symmetric situation, $\frac{\partial^2 c}{\partial \theta^2} = 0$. Then, writing the time derivative in forward difference and the spatial derivatives in central differences gives:

$$c_i^{t2} = c_i^{t1} + \frac{D_e \Delta t}{(\Delta r)^2} (c_{i+1}^{t1} - 2c_i^{t1} + c_{i-1}^{t1}) + \frac{D_e \Delta t}{2r_i \Delta r} (c_{i+1}^{t1} - c_{i-1}^{t1}) \quad (6)$$

The central difference equation with constant Δr is, in principle, 2nd order accurate, meaning that a grid-refinement by a factor of 2 should result in a solution that is 4 times more accurate. However, problems often appear at boundary cells where concentrations change abruptly, and the error there may propagate into the rest of the model in a complicated manner. It is shown by Appelo and Postma (2005, p. 545) that weighting the constant concentration twice in the difference equation correctly solves the constant concentration boundary condition.

The PHREEQC-2 manual (Parkhurst and Appelo, 1999) gives a more general equation for solving diffusion among cells of any form in the stagnant zones of a dual porosity medium that can be modeled by PHREEQC-2:

$$c_i^{t2} = c_i^{t1} + D_e \Delta t \sum_{j \neq i}^n \frac{A_{ij}}{h_{ij} V_i} (c_j^{t1} - c_i^{t1}) f_{bc} \quad (7)$$

where A_{ij} is the shared surface area among cells i and j (m²), h_{ij} is the distance between midpoints of the cells (m), V_i is the volume of cell i (m³), and f_{bc} is a correction factor for boundary cells. Equation (7) can be derived, writing out Fick's first law for cell i and solving the mass balance (cf. Appelo and Postma, 2005, p. 87).

If the cells are built in concentric layers with equal spacing $h_{ij} = \Delta r$, then

$$\frac{A_{ij}}{V_i} = \frac{2(r_i + \Delta r / 2)}{2r_i \Delta r} \quad \text{for } j = i+1, \text{ and } \frac{A_{ij}}{V_i} = \frac{2(r_i - \Delta r / 2)}{2r_i \Delta r} \quad \text{for } j = i-1 \quad (8)$$

Substituting Equation (8) in (7), taking $f_{bc} = 2$ if j is a constant concentration cell and 1 otherwise, and further writing out, also produces Equation (6). Thus, radial diffusion can be modeled with PHREEQC-2 with 2nd order accuracy, using option ‘-stagnant’ of keyword TRANSPORT. A series of mixing factors must be defined with keyword MIX as explained in the PHREEQC-2 manual (p. 52, 251-253). In the terms of the finite difference formula (6), the mixing factors are:

$$mixf_{i+1} = \frac{D_e \Delta t (2r_i + \Delta r)}{2r_i (\Delta r)^2} \text{ and } mixf_{i-1} = \frac{D_e \Delta t (2r_i - \Delta r)}{2r_i (\Delta r)^2} \quad (9)$$

and Equation (6) becomes:

$$c_i^{t2} = mixf_{i+1} c_{i+1}^{t1} + mixf_{i-1} c_{i-1}^{t1} + (1 - mixf_{i+1} - mixf_{i-1}) c_i^{t1} \quad (10)$$

Equation (10) shows that c_i^{t2} becomes negative if $c_i^{t1} > 0$, $c_{i\pm 1}^{t1} = 0$, and $(mixf_{i+1} + mixf_{i-1}) > 1$. Accordingly, the timestep Δt must be constrained to the maximum that keeps $(mixf_{i+1} + mixf_{i-1}) < 1$ in the grid, and $(mixf_{i+1} + 2 mixf_{i-1}) < 1$ in any of the cells in contact with a constant concentration. This timestep condition also prevents numerical oscillations in most situations (Appelo and Postma show that $(mixf_{i+1} + 2 mixf_{i-1}) < 2/3$ will *always* prevent oscillations).

Similar to the radial grid, mixing factors can be calculated for the elliptical grid needed for modeling Wersin *et al.*'s experiment.

5.2. Modeling tritium, iodide and sodium from the experimental data

The porewater diffusion coefficient is the parameter to be fitted on the concentration data from the diffusion experiment. The porewater diffusion coefficient is related to the effective diffusion coefficient used above in Fick's law (Equation 5) and to the solute's tracer diffusion coefficient in ‘free’ water by,

$$D_{e,i} = \frac{\varepsilon_{a,i}}{R_i} D_{p,i} = \frac{\varepsilon_{a,i}}{R_i} \frac{D_{w,i}}{\theta_i^2} \quad (11)$$

where $D_{e,i}$ is the effective diffusion coefficient for solute i (m^2/s), $\varepsilon_{a,i}$ is the accessible porosity (-), R_i is the retardation (-), $D_{p,i}$ is the porewater diffusion coefficient (m^2/s), $D_{w,i}$ is the tracer diffusion coefficient in water (m^2/s), and θ_i is the tortuosity (-). The retardation is, in principle, calculated by the geochemical model; for $^{22}Na^+$ it is defined by the cation exchange capacity and the porewater composition of the Opalinus Clay, tritium and iodide are not retarded ($R = 1$). The accessible porosity is the water-filled porosity for tritium and Na^+ ($\varepsilon_a = 0.16$), and half of that for iodide. (The accessible porosity is found by comparing porewater concentrations with concentrations in the ‘free’ solution that contacts the clay, or by combining the transient and steady states in a laboratory diffusion experiment (Van Loon *et al.*, 2004)).

The tracer diffusion coefficients are known, mainly from measured electrical conductivities (Robinson and Stokes, 1959). The smaller accessible porosity for iodide is incorporated in the model by defining half of the porewater to be DDL water. Thus, the tortuosity is the only remaining parameter that is ‘free’ to be fitted. Computed and measured concentrations in the borehole fluid are compared in Figure 11, using the tortuosity that is optimized for tritium (full line for tritium, dotted lines for iodide and sodium), or optimized tortuosities for iodide and sodium (full lines) (Appelo and Wersin, 2007).

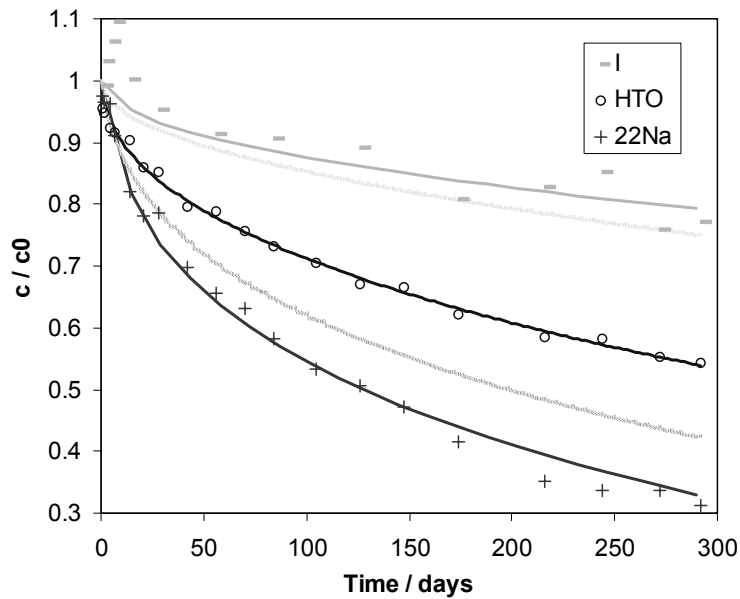


Figure 11. Observed iodide, tritium and sodium in the borehole fluid during an *in-situ* diffusion experiment in Opalinus Clay (symbols) and model calculated concentrations (lines) in Mont Terri experiment. The dotted lines stem from a model in which tritium, iodide and sodium have the same tortuosity. The full line for iodide results when the tortuosity is increased by 1.2. The full line for ^{22}Na is obtained with a 1.5 times smaller tortuosity than of tritium (Appelo and Wersin, 2007).

The tortuosity of iodide is *higher* than of tritium. It can be explained by the heterogeneous distribution of clay minerals which creates a spatially variable diffuse double layer that blocks transport of the anions in pore constrictions where cations and tritium can continue to diffuse. The tortuosity of $^{22}\text{Na}^+$ is *smaller* than of tritium. This is more difficult to explain, and may be a result of diffusion through the interlayer space of swelling clay minerals, or perhaps of surface diffusion of exchangeable cations.

6. CONCLUSIONS

Version 2.13 of the PHREEQC hydrogeochemical code was extended with multicomponent diffusion and diffuse double layer diffusion for comprehensive modeling of transport in clays. The code can handle laboratory and *in-situ* diffusion experiments in a way not possible hitherto. Examples of multicomponent diffusion were discussed, showing 1) uphill diffusion as a result of different diffusion speeds of individual ions, a process that cannot be explained by Fickian diffusion, 2) precipitation reactions that can only be modeled correctly with kinetic rates, 3) precipitation of scheelite in a laboratory diffusion experiment, and 4) an *in-situ* diffusion experiment in Opalinus Clay where diffusion data of tritium, $^{22}\text{Na}^+$ and I^- were modeled altogether in an elliptical grid.

Acknowledgements

The PHREEQC input files for the cases presented are available on request to appt@xs4all.nl. Paul Wersin aroused my interest in the Opalinus Clay experiments, and so incited the adaptations of PHREEQC reported here.

REFERENCES

Appelo, C.A.J. and Postma, D. (2005): *Geochemistry, groundwater and pollution*, 2nd ed. Balkema, Leiden, 649 pp.

- Appelo, C.A.J. and Wersin, P. (2007): Multicomponent diffusion modeling in clay systems with application to the diffusion of tritium, iodide and sodium in Opalinus Clay. *Environ. Sci. Technol.* 41, 5002-5007.
- Ben-Yaakov, S. (1972): Diffusion of seawater ions into dilute solution. *Geochim. Cosmochim. Acta*, 36: 1396-1406.
- Boudreau, B.P., Meysman, F.J.R., and Middelburg, J.J. (2004): Multicomponent ionic diffusion in porewaters: Coulombic effects revisited. *Earth Planet. Sci. Lett.*, 222: 653-666.
- Cussler, E.L. (1984): *Diffusion - mass transfer in fluid systems*. Cambridge UP, 525 pp.
- Lichtner, P.C. (1995): Principles and practice of reactive transport modeling. *Mat. Res. Soc. Symp. Proc.*, 353: 117-130.
- Parkhurst, D.L. and Appelo, C.A.J. (1999): *User's guide to PHREEQC* (version 2). U.S. Geol. Surv. Water Resour. Inv. Rep. 99-4259, 312 pp.
- Pina, C.M., Fernández-Díaz, L. and Astilleros, J.M. (2000): Nucleation and growth of scheelite in a diffusing-reacting system. *Cryst. Res. Technol.*, 35: 1015-1022.
- Prieto, M., Putnis, A. and Fernández-Díaz, L. (1990): Factors controlling the kinetics of crystallization: supersaturation evolution in a porous medium. *Geol. Mag.*, 127: 485-495.
- Prieto, M., Fernández-González, A., Putnis, A. and Fernández-Díaz, L. (1997): Nucleation, growth, and zoning phenomena in crystallizing (Ba, Sr)CO₃, Ba(SO₄, CrO₄), (Ba, Sr)SO₄ and (Cd, Ca)CO₃ solid solutions from aqueous solutions. *Geochim. Cosmochim. Acta*, 61: 3383-3397.
- Robinson, R.A. and Stokes, R.H. (1959): *Electrolyte solutions: the measurement and interpretation of conductance, chemical potential and diffusion in solutions of simple electrolytes*. Butterworths, London.
- Sato, H., Ashida, T., Kohara, Y., Yui, M. and Sasaki, M. (1992): Effect of dry density on diffusion of some radionuclides in compacted sodium bentonite. *J. Nucl. Sci. Technol.*, 29: 873-882.
- Van Loon, L.R., Soler, J.M., Müller, W. and Bradbury, M.H. (2004): Anisotropic diffusion in layered argillaceous formations: a case study with Opalinus clay. *Environ. Sci. Technol.*, 38: 5721-5728.
- Vinograd, J.R. and McBain, J.W. (1941): Diffusion of electrolytes and of the ions in their mixtures. *J. Am. Chem. Soc.*, 63: 2008-2015.
- Wersin, P., Van Loon, L.R., Soler, J.M., Yllera, A., Eikenberg, J., Gimmi, Th., Hernán, P. and Boisson, J.Y. (2004): Long-term diffusion experiment at Mont Terri: first results from field and laboratory data. *Applied Clay Sci.*, 26: 123-135.